

Anisotropic Thermal Expansion and Cooperative Invar/Anti-Invar Effects in MnNi Alloy

Thermal expansion of a tetragonal $\text{Mn}_{88}\text{Ni}_{12}$ alloy, which exhibits significant anisotropy, was investigated by EXAFS and path-integral quantum mechanical simulations. The EXAFS reveals that the Mn local environment is actually tetragonally distorted, while the Ni one retains its inherent cubic-like symmetry. The large thermal expansion along the a axis originates from the anti-Invar effect, while the negligibly small thermal expansion along the c axis originates from the cooperative Invar effect. Namely, the tetragonally distorted more stable antiferromagnetic Mn state gives a significantly smaller (slightly longer) atomic radius along a (c) than that of the spherical paramagnetic state.

An Invar alloy $\text{Fe}_{66}\text{Ni}_{34}$ that shows anomalously small thermal expansion over a wide temperature range was discovered by Guillaume in 1897 [1]. The Invar effect has been utilized in various kinds of precision devices and instruments such as semiconductor and flat-panel-display manufacturing systems, molded imprints, astronomical telescopes and so forth. In a phenomenological model of the Invar effect, there exist at least two types of electronic states in Fe, typically called high-spin (HS) and low-spin (LS) states [2]. In this two-state model, the HS state with a larger atomic radius is slightly more stable at a temperature of 0 K than the LS state. This results in the compensation of thermal expansion due to increasing density of the LS state at higher temperature. However, the detailed origin of the Invar effect is the subject of much discussion even today. In recent electronic structure calculations based on the density-functional theory [3], a much more complicated electronic structure was proposed, where non-collinear magnetic moments with different magnitudes are distributed, depending on the local environment. On the other hand, the thermal expansion was very recently investigated from a different viewpoint of thermal vibration, by com-

paring temperature-dependent EXAFS measurements with the path integral effective classical potential (PIECP) Monte-Carlo (MC) simulations [4]. In this work, cooperative anisotropic thermal expansion in face-centered tetragonal (fct) $\text{Mn}_{88}\text{Ni}_{12}$ alloy was studied, where one axis shows the Invar effect and the other shows the anti-Invar effect [5].

In this work, we performed temperature-dependent Mn and Ni K-edge EXAFS measurements at BL-9C using the transmission mode. The temperature range of the EXAFS measurements was 11–300 K. Powder XRD measurements were also performed by using laboratory equipment. The 113 and 311 diffractions were mainly used to determine the fct lattice constants a and c .

Figure 1 gives the bond distances around Mn and Ni determined by EXAFS. The analysis clearly shows that the environment around Mn is really tetragonally distorted with meaningfully different bond distances between $\text{Mn}(l)$ and $\text{Mn}(s)$. On the other hand, the environment around Ni is regarded as cubic because of a negligible difference between $\text{Ni}(l)$ and $\text{Ni}(s)$. It should be noted here that in spite of the fact that the average X-ray structure is fct, the local structures of Mn and Ni

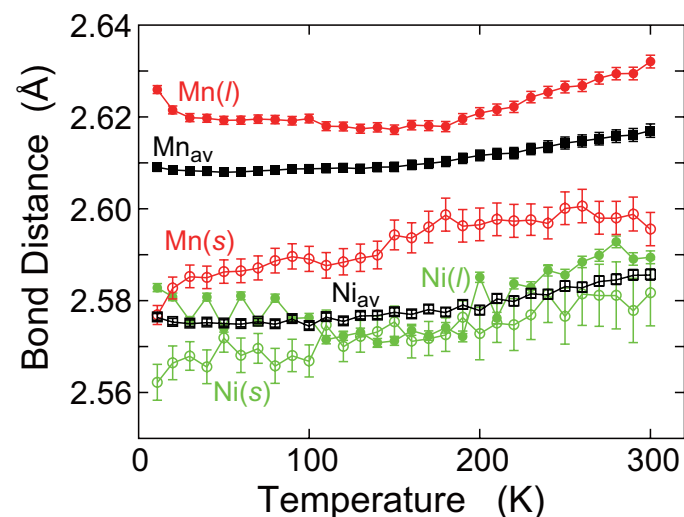


Figure 1: Experimental bond distances in $\text{Mn}_{88}\text{Ni}_{12}$ determined by Mn and Ni K-edge EXAFS. l , s , and av denote the longer and shorter bonds and the average, respectively.

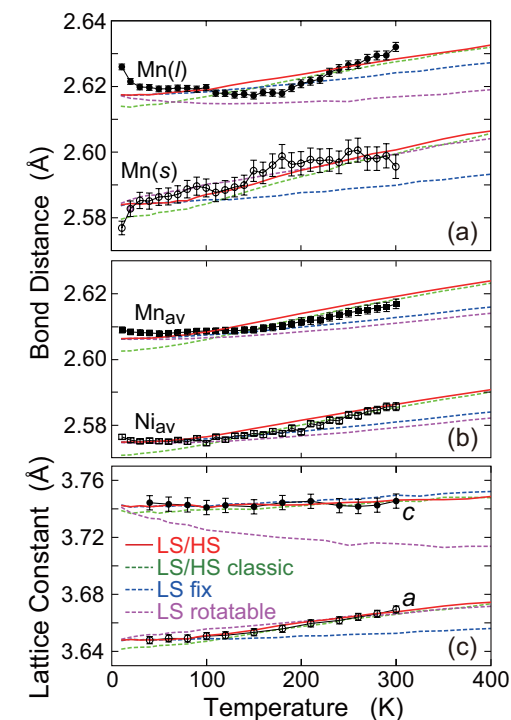


Figure 2: Simulated bond distances for (a) $\text{Mn}(l)$ and $\text{Mn}(s)$ and (b) Mn_{av} and Ni_{av} , and (c) fct lattice constants a and c , together with the experimental EXAFS and XRD data with error bars. Four kinds of simulated results are depicted: the quantum LS-HS model (red solid line), the classic LS-HS model (green dashed), the tetragonal-axis fixed LS model (blue dashed), and the tetragonal-axis rotatable model (purple dashed).

determined by EXAFS are essentially different. Figure 2 gives the experimental and PIECP-simulated results for the bond distances and the lattice constants. In the lattice constants in Fig. 2(c), a ($a < c$) shows somewhat larger thermal expansion than usually expected, while the lattice constant c exhibits almost no thermal expansion, indicating cooperative Invar/anti-Invar effects. It is clearly found that in the PIECP simulations, the LS/HS two-state model successfully reproduces all the experimental lattice constants and bond distances. In the tetragonal-axis rotatable LS model, the calculated lattice constant c gradually decreases with temperature, while the experiment shows nearly no thermal expansion. In the tetragonal-axis fixed LS model, where only the Mn LS state is allowed and the Mn axis is fixed at [001], thermal expansion of the lattice constant a is estimated to be too small compared to the experiments. The classic LS/HS model is rather good, but the lattice constants are erroneously temperature dependent even at low temperature, implying the importance of the vibrational quantum effect. In the quantum mechanical LS/HS model, the bond distances as well as the lattice constants agree quite well with the experimental results. This confirms that the two inequivalent bonds in EX-

AFS are regarded as the bonds within the bc/ca and ab planes. Consequently, the present anisotropic thermal expansion is explained by the cooperative Invar/anti-Invar effects in the Mn atom, where the tetragonally distorted more stable LS Mn state gives a smaller atomic radius within the ab plane and a larger radius along the c axis than the spherical one of the HS state.

In summary, the fct lattice constant a ($a < c$) shows somewhat larger thermal expansion than usual, while the lattice constant c exhibits almost no thermal expansion. This behavior is explained by the cooperative Invar/anti-Invar effects in the Mn atom, where the tetragonally distorted Mn state coupled antiferromagnetically to the neighboring atoms is more stable than the spherical paramagnetic HS state and as a result, gives a significantly smaller atomic radius within the ab plane and a slightly larger radius along the c axis than the spherical one of the HS state. The present observation is not a rare case; similar thermal expansion behaviors can be seen in $\text{Mn}_{87}\text{Pd}_{13}$ and $\text{Mn}_{85}\text{Zn}_{15}$, although they have not been discussed so far. Mn atoms are tetragonally distorted associated with the lattice distortion, while Ni atoms retain cubic symmetry. From the local point of view, it is not unusual that different structural behaviors in randomly distributed different elements are observed. It should be noted that XRD gives only the average structure and the local structure is not always the same in random alloy/solid solution systems. Recently, there have been reports on several kinds of metal alloys that exhibit anomalous thermal expansion properties like negative or zero thermal expansion. Since these works have focused on the lattice thermal expansion, it will be interesting to investigate the thermal expansion from the present viewpoint of local thermal expansion.

REFERENCES

- [1] C.E. Guillaume, *C. R. Acad. Sci.* **125**, 235 (1897); E.F. Wasserman, *Ferromagnetic Materials*, edited by K.H.J. Bushow and E.P. Wohlfarth (Elsevier Science Publishers B.V., 1990). Vol. 5, 237.
- [2] R.J. Weiss, *Proc. R. Soc. Lond. A* **82**, 281 (1963).
- [3] M. van Schilfgaarde, I.A. Abrikosov and B. Johansson, *Nature* **400**, 46 (1999).
- [4] T. Yokoyama and K. Eguchi, *Phys. Rev. Lett.* **107**, 065901 (2011).
- [5] T. Yokoyama and K. Eguchi, *Phys. Rev. Lett.* **110**, 075901 (2013). This work was introduced as an IMSS topic in <http://imss.kek.jp/news/2013/topics/0207invar/index.html> and also in Japanese newspapers of *Nikkan Kogyo Shimbun* (Feb. 8, 2013) and in *Kagaku Shimbun* (Feb. 22).

BEAMLINE
BL-9C

T. Yokoyama^{1,2} and K. Eguchi² (¹IMS, ²The Grad. Univ. for Adv. Stud.)